Isolation and Characterization of a Pseudorabies Virus Variant Strain in Gansu Province, China, 2021

Xiaobing He , Hua Yang , Peng Ji , Guohua Chen , Yongxiang Fang , Zhizhong Jing , Yanming Wei *

Posted Date: 21 April 2025

doi: 10.20944/preprints202503.1223.v2

Keywords: pseudorabies virus; variant strain; biological characteristics; genetic evolution; pathogenicity; Gansu Province

 doi:10.20944/preprints202503.1223.v2

Article

Isolation and Characterization of a Pseudorabies Virus Variant Strain in Gansu Province, China, 2021

Xiaobing He [1,2,3,4], Hua Yang [5], Peng Ji [1], Guohua Chen [2,3,4], Yongxiang Fang [2,3,4], Zhizhong Jing [2,3,4] and Yanming Wei [1,*]

[1] College of Veterinary Medicine, Gansu Agricultural University, Lanzhou 730070, China
[2] State Key Laboratory for Animal Disease Control and Prevention, Lanzhou Veterinary Research Institute, Chinese Academy of Agricultural Sciences, Lanzhou 730046, China
[3] Gansu Province Research Center for Basic Disciplines of Pathogen Biology, Lanzhou 730046, China
[4] Key Laboratory of Veterinary Etiological Biology and Key Laboratory of Ruminant Disease Prevention and Control (West), Ministry of Agricultural and Rural Affairs, Lanzhou 730046, China
[5] Gansu Vocational College of Agriculture, Lanzhou 730030, China
* Correspondence: weiym@gsau.edu.cn

Abstract: The outbreaks of pseudorabies (PR) caused by pseudorabies virus (PRV) variant strains have led to huge economic losses in the pig industry in China in recent years. In this study, a variant PRV strain named PRV/Gansu/China/2021 (GS-2021) was successfully isolated and identified from brain tissue samples of PR-suspected dead piglets at a Bartha-K61-vaccinated pig farm in Gansu Province, China in 2021. Its biological characteristics, genetic features, evolutionary relationship, and pathogenicity were further evaluated. The results indicate that the PRV GS-2021 strain had different plaque sizes but no significant difference in replication kinetics from the Bartha-K61 strain *in vitro*. In addition, sequence alignments revealed that the gB, gC, gD, and gE proteins of the PRV GS-2021 strain share high homology with those of the Chinese variant strains. However, glutamate is replaced by glycine at position 91 and two aspartate insertions are detected at sites 48 and 496 in the gE protein of the virus. Phylogenetic analysis revealed that it was more closely related to endemic PRV strains, particularly the variant strains circulating in China, based on the *gB*, *gC*, *gD*, and *gE* genes and complete genome sequence. Moreover, we further discovered that the PRV GS-2021 strain exhibited a higher pathogenicity than the Bartha-K61 strain in mice through analyses of mortality, histopathology, and viral loads. Overall, our results suggest that the isolated PRV GS-2021 strain, as a variant with higher virulence and pathogenicity, was prevalent in Gansu Province, China before 2021. These findings are important for continuously monitoring the epidemiological characterization and genetic evolution of PRV, providing useful guidance for the design of novel vaccines and more efficacious control and prevention strategies for PR in the future.

Keywords: pseudorabies virus; variant strain; biological characteristics; genetic evolution; pathogenicity; Gansu Province

1. Introduction

Pseudorabies virus (PRV) is also known as Aujeszky's disease virus or Suid herpesvirus type 1 and belongs to the genus *Varicellovirus* in the subfamily *Alphaherpesvirinae* of the family *Herpesviridae*. PRV is an enveloped virus with a large double-stranded linear DNA genome approximately 150 kb in length, encoding at least 70 proteins [1]. PRV is the causative agent of Pseudorabies (PR) and has the capacity to infect a wide variety of wildlife, domestic animals, and livestock, including ruminants, carnivores, and rodents. However, pigs constitute the natural reservoir for PRV and can become latent carriers, leading to acute infection and great economic losses in the swine industry worldwide, particularly in developing countries [2–5]. PRV is a highly neurotropic virus that causes neurological

 doi:10.20944/preprints202503.1223.v2

disorders and frequently results in a high rate of mortality in newborn piglets [1,6]. Conversely, older pigs usually exhibit sub-clinical symptoms, such as respiratory disturbance, malaise, and decreased appetite [1,6]. Furthermore, PRV infections in pregnant sows may lead to breeding obstacles, including stillbirths, abortions, and weakling piglets [1,6]. Following the acute stage of infection, PRV can establish a latent infection that persists throughout the life of the infected pig. However, it is noteworthy that latently infected pigs can be re-infected due to the spontaneous reactivation of the latent viral genome or reactivation triggered by stress. This phenomenon weakens the immune system of latently infected pigs, thereby facilitating more severe infections [1].

In China, PR was effectively mitigated through the implementation of extensive vaccination programmers in swine populations by the extensive use of inactivated and live-attenuated vaccines, including Bartha-K61, SA215, and HB-98 [7–11]. However, by the conclusion of 2011, a significant resurgence of PR outbreaks had occurred on numerous Bartha-K61-vaccinated swine farms, rapidly disseminating to various regions across China and resulting in substantial economic losses [12–14]. A large number of research found that the Bartha-K61 vaccine strain was incapable of providing complete protection against new emerging PRV variant strains in China [10–23]. Genetic analysis revealed several mutations in most viral proteins of the PRV variants, including substitutions, insertions, and/or deletions [19–21]. These findings indicated that the emerging PRV variant strains had begun to circulate among populations of infected pigs in China. Meanwhile, some studies have indicated that increased virulence and antigenic variation of the novel PRV mutant strains are the primary causes of the serious spread in China, which could explain why there have been large-scale outbreaks of the emerging PRV variants in China since late 2011 [13–15,19–24]. Nonetheless, some other studies showed that the Bartha-K61 vaccine strain could protect pigs against acute lethal variant PRV infection [25–28]. Therefore, the controversy about whether Bartha-K61 could have preventive efficacy in protecting pigs against the PRV variant strains needs to be further evaluated. Furthermore, five licensed inactivated and live-attenuated vaccines based on PRV HeN1201, PRV C, PRV JS-2012, and PRV HeN1 strains revealed effective protection against PRV variant infections [17,29–32]. Recently, some novel recombinant PRV strains derived from different PRV genotypes or wild PRV strains and classical vaccines were isolated in China [33–41]. Notably, more than 30 clinical cases of PRV infection in humans so far have been reported in China [19–21,42–49]. Moreover, a human-originated PRV variant strain, designated as hSD-1/2019, was successfully isolated from a patient with cerebrospinal fluid in 2019 [19–21,50,51]. This provided direct evidence of PRV infection in humans, thus classifying the PRV variant strain as an emerging zoonotic pathogen. However, epidemiological data, genomic characterization, evolutionary relationship, and information regarding the pathogenicity of the PRV variant strains currently circulating in domestic pig populations in China, especially in Gansu Province, remain limited.

In the present study, a PRV variant strain, designated as PRV/Gansu/China/2021, was isolated and identified from a PR-suspected brain tissue from deceased piglets on a Bartha-K61-vaccinated pig farm in Gansu Province, China in 2021, and further investigation was conducted to ascertain the biological characteristics, genetic features and evolution, and pathogenicity of this strain in mice.

2. Materials and Methods

2.1. Cells, Viruses, Antibodies, and Animals

The propagation or titration of the virus was carried out in Vero cells (SCSP-520, CAS, China) and PK-15 cells (CCL-33, ATCC, USA) with Dulbecco's modified Eagle medium (DMEM) (11995073, Gibco, China) containing 10% fetal bovine serum (10091148, Gibco, New Zealand) at 37 ◦C in 5% CO2. The PRV vaccine strain Bartha-K61 was isolated from a commercial vaccine and used as a control virus, while brain tissue from specific pathogen-free (SPF) piglets was used as a negative control. The primary antibodies employed in this study were rabbit anti-pseudorabies virus gB antiserum (PSRVGB11-S, Alpha Diagnostic International, USA) and rabbit anti-pseudorabies virus antibody (ab3534, Abcam, USA). The secondary antibodies employed were goat anti-rabbit IgG alexa fluor®488 (H+L) (GB25303, Servicebio, China) and goat anti-rabbit IgG alexa fluor®594 (H+L)

 doi:10.20944/preprints202503.1223.v2

(GB28301, Servicebio, China). Adult BALB/c mice (6–8 weeks, 16–20 g body weight) from the Animal Experimental Center of the Lanzhou Veterinary Research Institute, Chinese Academy of Agricultural Sciences were also used.

2.2. Clinical Sample Collection and Virus Detection

Clinical brain samples were obtained from PRV-suspected dead piglets on a Bartha-K61-vaccinated pig farm in Gansu Province, China, in 2021. The brain samples were then homogenized in DMEM at 4 °C, after which the DNA was extracted using a Viral DNA Extraction Kit (9766, TaKaRa, Japan). The primers for the partial *gB* and *gE* gene fragments of PRV were designed according to reference strain (GenBank accession number: KJ789182). The amplified fragments of the target genes were 282 bp and 258 bp, respectively. The extracted DNA samples were identified with polymerase chain reaction (PCR) using PRV gB- and gE-specific pair primers (Table 1). The PCR products were then subjected to agarose gel electrophoresis to confirm their identity.

Table 1. Primers used in this study.

Gene	Primer Sequence （5' - 3'）	Length
gB	TGTACCTGACCTACGAGGCGTCATG GTGGGAGCCGTCACACGCGCCAGC	2818 bp
gC	TGTGTGCCACTAGCATTAAATCCGTT GTTCAACGCGCGGTCGTTTATTGAT	1605 bp
gD	ATACACTCACCTGCCAGCGCCATG ACCATCATCATCGACGCCGGTACT	1262 bp
gE	GTTGAGACCATGCGGCCCTTTCT GGACCGGTTCTCCCGGTATTTAAG	1786 bp
gB	TGCCCACGCACGAGGACTACTACG CGCCATAGTTGGGTCCATTCGTCAC	258 bp
gE	TGCAGAACAAGGACCGCACCCTGT GCGAGATGAGGAGCTCGTTGTCGT	282 bp
gB	AAGTTCAAGGCCCACATCT TGAAGCGGTTCGTGATGG FAM-CAAGAACGTCATCGTCACGACCG-BHQ	88 bp

2.3. Viral Isolation and Identification

PRV PCR gB- and gE-positive homogenates were treated with antibiotics and subjected to a centrifugation process at 5000 g/min for 15 min at 4 °C. Subsequently, the resultant filtrate was filtered through a 0.45 μm filter (0000240486, Merck Millipore, Germany) and inoculated into a monolayer of Vero cells. The cells were then incubated in Minimum Essential Medium (MEM) (11095080, Gibco, USA) with 1% FBS in a 5% CO2 incubator at 37 °C. The presence of a cytopathic effect (CPE) was examined daily, and the observation of cell morphology and the anchorage-dependent rate were recorded using a microscope. At 85-95% CPE, the Vero cells were subjected to freeze-thaw cycles with the culture medium, after which the cell culture medium was collected. Following amplification, cultivation, and six rounds of plaque purification, the virus was identified using indirect immunofluorescent assay (IFA) and transmission electron microscope (TEM) system HT7800 (Hitachi, Japan), PCR and Sanger sequencing.

2.4. Plaque Assay and Plaque Size Determination

Vero cells were seeded in 12-well plates, after which a serial 10-fold dilution of the virus was added to the cells. Following a one-hour incubation period, the cells were washed three times with PBS and overlaid with 0.75% carboxy methyl cellulose (M352, Fisher Scientific, USA) in DMEM medium containing 2% FBS. The plates were then incubated at 37 °C for 2–3 days until visible plaques formed. The cells were then fixed using 4% paraformaldehyde (252549, Sigma-Aldrich, USA) and

 doi:10.20944/preprints202503.1223.v2

then stained with 500 µl of crystal violet (C0775, Sigma-Aldrich, USA). The plaque-forming units (PFUs) of the isolated PRV GS-2021 strain were then calculated by plaque assay. A total of 50 plaques of each virus were randomly selected, and their diameters were measured using the Image J software. The relative diameter of the plaque was then calculated as the product of the diameter of the PRV GS-2021 strain divided by those of the Bartha-K61 strain.

2.5. One-Step Growth Curve of the PRV GS-2021 Strain

Vero cell monolayers in 12-well plates were infected with the virus at an MOI of 1. Following incubation at 37 °C for 1 hour, the medium was replaced with DMEM containing 2% FBS. The cells and the remaining fluid were harvested at 6-, 12-, 24-, 36-, and 48-hour post-infection (hpi) and stored in aliquots at −80 °C. Following three freeze-thaw cycles, the virus was titrated using the plaque formation assay in Vero cells.

2.6. Amplification and Sequencing of gB, gC, gD, and gE Genes of the PRV GS-2021 Strain

The complete *gB*, *gC*, *gD*, and *gE* genes of the PRV strain were amplified by PCR through specific primers (Table 1). The PCR reaction was conducted in a 100 µl volume containing 20 ng of extracted DNA, 20 µl of 5 × PrimeSTAR GXL Buffer, 2 µl of PrimeSTAR GXL DNA polymerase (R050A, TaKaRa, China), 8 µL of 2.5 mM deoxynucleoside triphosphate (dNTP), 0.25 µM of each primer, and nuclease-free water to bring the total volume to 100 µl. The thermal cycling parameters were 95 ℃ for 4 sec, then 35 cycles of denaturation at 98 ℃ for 10 sec, annealing at 55 ℃ for 10 sec, and extension at 68 ℃ for 3 min 20 sec, followed by a final extension at 72 ℃ for 10 min. The purified PCR products were connected to the pJET1.2 vector with the Clone JET PCR Cloning Kit (K1231, Thermo Scientific, USA) and verified through sequencing to obtain the final assembly results.

2.7. Complete Genome Sequencing of the PRV GS-2021 Strain

The whole genome sequence of the purified PRV GS-2021 strain was according to the manufacturer's instruction of the Viral DNA Extraction Kit (9766, TaKaRa, Japan). Purified genomic DNA was sequenced through next-generation sequencing (NGS) technology using the high-throughput Nova 6000 Illumina platform (Magigen Biotech, Guangzhou, China). Paired-end 150-bp reads were generated from libraries with an insert size of 350 bp. Illumina genomic reads of each accession were used as the input of the Jellyfish tool 60 to obtain the k-mer frequency for estimating genome size. Approximately 2-Gb clean reads of 2 × 100 bp pair-ends from the library averaging 400 bp in size were obtained for PRV.

Raw reads were cleaned by filtering the low-quality reads using Soapnuke (v2.0.5). Host reads were removed using BWA (v0.7.17). The cleaned reads were mapped to the PRV sequence database downloaded from GenBank (Accession number: KJ789182) (Table 2). Reference-based assembly was performed using BWA (v0.7.17), samtools (v0.7.17), and blast (v2.9.0), respectively. To correct reference assembly errors such as indels and mismatches, de novo assembly was executed using BWA (v0.7.17), samtools (v0.7.17), and bcftools (v1.8), respectively. Integrating the results of the reference-based assembly and the de novo assembly, the final assembly sequence was obtained.

Table 2. Information of PRV reference strains used in this study.

Strain	Accession Number	Genotype	Country	Isolation Date
TJ	KJ789182	IIb	China	2012
HeN1	KP098534	IIb	China	2012
JS-2012	KP257591	IIb	China	2012
HLJ8	KT824771	IIb	China	2013
GD-YH	MT197597	IIb	China	2014
HN1201	KP722022	IIb	China	2015
JS-XJ5	OP512542	IIb	China	2016

 doi:10.20944/preprints202503.1223.v2

HeNZM	MT775883	IIb	China	2017
JSY7	MT150583	IIb	China	2018
FJ	MW286330	IIb	China	2019
hSD-1	MT468550	IIb	China	2019
SD18	MT949536	IIb	China	2020
JM	OK338077	IIb	China	2021
CD22	OR666765	IIb	China	2022
HLJPRVJ	OR365764	IIb	China	2023
HLJ-2013	MK080279	IIa	China	2013
JS-2020	OR271601	IIa	China	2020
SC	KT809429	IIa	China	1986
Ea	KU315430	IIa	China	1990
Fa	KM189913	IIa	China	2012
Kolchis	KT983811	I	Greece	2010
Bartha	JF797217	I	Hungary	1960
Kaplan	JF797218	I	Hungary	2011
Becker	JF797219	I	USA	1967
NIA3	KU900059	I	UK	2016

2.8. Phylogenetic Analyses of the PRV GS-2021 Strain

Twenty-five genome sequences of PRV representing wild strains or vaccine strains from different endemic countries were obtained from GenBank (Table 2). The sequence of the PRV GS-2021 strain was compared to those of viral strains from different endemic countries. The alignment of the nucleic acid and amino acid sequences was conducted using a MegAlign module in the DNASTAR Lasergene. v7.1 software. Phylogenetic trees were also calculated using the maximum-likelihood method in the MEGA-X software based on the following substitution models: the general time-reversible model for the *gB* gene sequences, the general time-reversible model with invariant sites for the *gC* gene sequences, the hasegawa-kishino-yano with invariant sites substitution model for the *gD* gene sequences, the general time-reversible model for the *gE* gene sequences, and the general time-reversible model with gamma distribution for the complete genomic sequences, and 1000 bootstrap replication.

2.9. Challenge of Mice with the PRV GS-2021 Strain

For the pathogenicity of the PRV GS-2021 strain, 24 specific pathogen-free (SPF) BALB/c mice were intranasally injected with 10^4, 10^3, and 10^2 PFU of the variant strain in 10 μl DMEM per mice. At the same time, 32 mice were designated as controls and injected with 10^6, 10^5, and 10^4 PFU of the Bartha-K61 strain 10 μl DMEM per mice and an equivalent volume of DMEM. After inoculation, the mice were observed each day for clinical symptoms and death, and the median lethal dose (LD50) of the virus strains was calculated using the Spearman–Karber method. Liver, spleen, lung, brain, and/or blood were collected from the GS-2021 and Bartha-K61-infected mice on the 3rd day post-infection for hematoxylin and eosin (H&E) staining and IFA, and the virus was detected using gB-specific TaqMan quantitative PCR (Table 1).

2.10. Statistical Analysis

The data were presented as the means ± standard errors of the means from three independent assays. Statistical analyses were performed using the GraphPad Prism version 5.0 software. The significance of the differences among the groups was evaluated using Student's t-test or two-way analysis of variance. A p-value of less than 0.05 was considered statistically significant: ∗∗∗, $p<0.01$; ∗∗∗, $p<0.001$, and ∗∗∗∗, $p<0.0001$.

3. Results

 doi:10.20944/preprints202503.1223.v2

3.1. Detection of PRV in Clinical Brain Tissue using PCR

Sick piglets from one farm in Wuwei (Gansu Province, China) presented with multiple clinical signs, including high fever (≥40.5 °C), depression, inappetence, weight loss, dyspnea, chilling, vomiting, secretion discharged from mouth, and systemic neurological symptoms. Viral genome DNA was extracted from clinical brain tissue samples, and the partial *gB* gene and *gE* gene of PRV were amplified using the PCR method. As shown in Figure 1, the PRV-suspected brain samples were verified to be positive for the *gB* and *gE* genes. However, the *gE* gene was negative for the PRV Bartha-K61 genome (used as a positive control) and for the brain sample from a healthy piglet (used as a negative control). This suggests that the dead piglets on the Bartha-K61-vaccinated farm were infected with the PRV field strain.

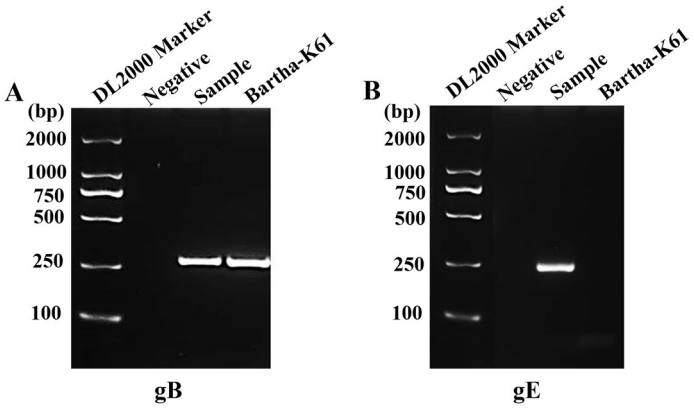

Figure 1. Detection of the PRV *gB* and *gE* genes in clinical brain samples using PCR. (**A**) Amplified PCR product of partial PRV *gB* gene (258 bp). (**B**) Amplified PCR product of partial PRV *gE* gene (282 bp). A negative sample from a specific pathogen-free (SPF) piglet was used as a negative control and Bartha-K61 was used as a positive control.

3.2. Isolation and Identification of the PRV GS-2021 Strain

The PRV gB - and gE-positive tissue samples were processed and inoculated into Vero cells. After 18 hours, a clear cytopathic effect (CPE) was observed, and characterized by cell shrinkage, reduced size, rounding, loose arrangement, and poor adhesiveness. These characteristics were similar to those of the Bartha-K61 strain with the PRV-positive homogenate (Figure 2A). In addition, the specific gB fluorescence signals were observed in the cytoplasm and nucleus of the PRV-infected Vero cells using IFA (Figure 2A). Meanwhile, herpesvirus-like virus particles were detected in the Vero cells infected with PRV isolate and Bartha-K61 using TEM (Figure 2B). The virus particles isolated through sucrose density-gradient centrifugation had a diameter of 81~161 nm and exhibited a spherical envelope protein with radially arranged spikes, as observed using TEM (Figure 2B). This is consistent with the morphology of PRV. However, there was no obvious difference in the morphology between the isolated PRV and the Bartha-K61 strain. Moreover, viral genome DNA was extracted from PRV, and the complete sequences of *gC* and *gE* genes still tested positive using PCR, which was further confirmed using Sanger sequencing (Figure 2C). These results indicate that a field PRV strain was successfully isolated from clinical samples from a Bartha-K61-vaccinated swine farm and named PRV/Gansu/China/2021 (also known as PRV GS-2021).

 doi:10.20944/preprints202503.1223.v2

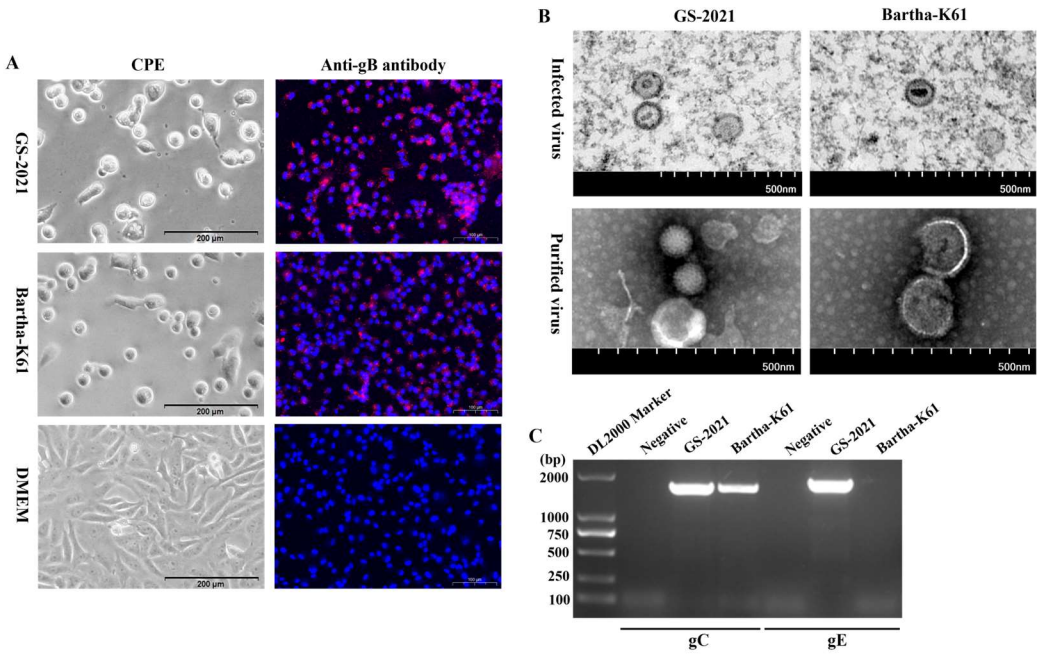

Figure 2. Isolation and identification of the PRV GS-2021 strain. (**A**) The cytopathic effect (CPE) of Vero cells caused by GS-2021 (left panels). An indirect immunofluorescence assay was used to detect gB (red color) protein in GS-2021 or Bartha-K61-challenged Vero cells, with the nucleus stained with DAPI (blue color) (right panels). (**B**) Viral particles in Vero cells (top panel) or purified virus (bottom panel) of GS-2021 and Bartha-K61 under a transmission electron microscope. (**C**) PCR amplification of PRV *gC* (1605 bp) and *gE* (1786 bp) fragments from passage 6 cultures of GS-2021-inoculated Vero cells. Bartha-K61 was used as a positive control, and DMEM was used as a negative control.

3.3. Biological Characteristics of the PRV GS-2021 Strain

Plaque assay and one-step growth curve experiments were performed to investigate the growth characteristics of the PRV GS-2021 strain, and the Bartha-K61 vaccine strain was used as a control group. The viral titers of the GS-2021 and Bartha-K61 were $1.15*10^7$ and $1.5*10^6$ PFU/ml, respectively. The GS-2021 strain developed a plaque area significantly larger than that of the Bartha-K61 strain (Figure 3A, B), suggesting a much stronger virus spread of the GS-2021 strain than that of the Bartha-K61 strain in Vero cells. Furthermore, one-step growth curve analysis revealed that the GS-2021 strain displayed similar growth kinetics and replication superiority at the end time point compared with the Bartha-K61 strain in Vero cells (Figure 3C). However, the Bartha-K61 strain propagated slightly faster than the GS-2021 strain in PK-15 cells (Figure 3D), which may be attributed to the better adaptation of Bartha-K61 to this cell line. These results show that the PRV GS-2021 strain exhibited different plaque sizes, but there was no significant difference in replication kinetics in Vero and PK-15 cells, compared to the Bartha-K61 strains.

 doi:10.20944/preprints202503.1223.v2

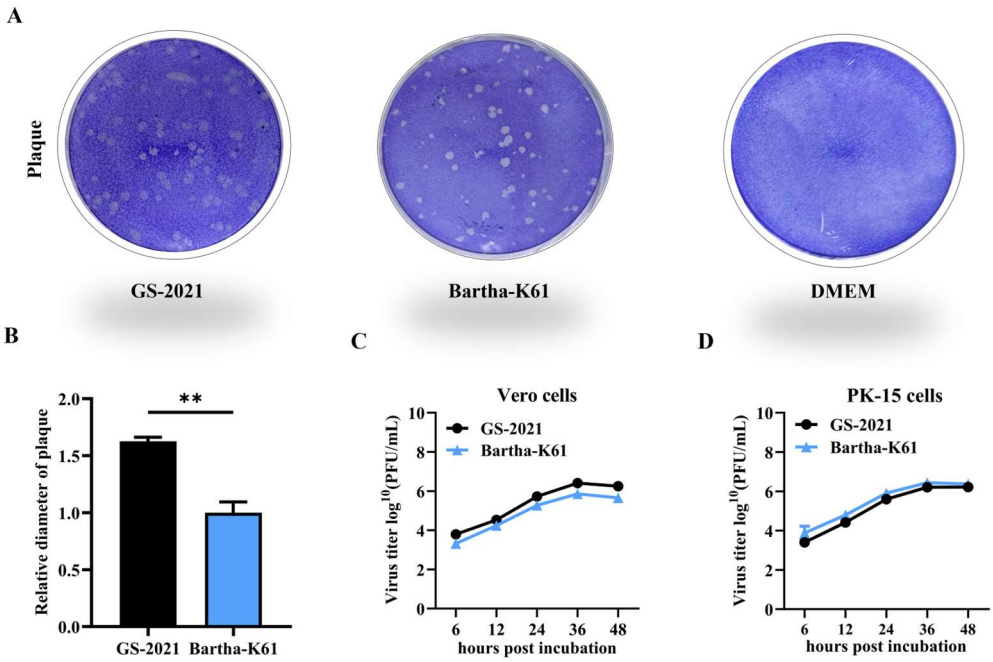

Figure 3. Biological characteristics of the PRV GS-2021 strain in vitro. (**A**) Plaque formation in Vero cells infected by GS-2021 and Bartha-K61. (**B**) The relative plaque size of each virus was normalized to that of Bartha-K61. Significant differences were considered: **P < 0.01. (**C, D**) One-step growth curves of the two PRV strains in Vero cells and PK-15 cells at an MOI of 1, respectively. The viral titers were determined in Vero cells using the plaque assay method.

3.4. Genetic Features of the PRV GS-2021 Strain

To identify the genetic characteristics of the PRV GS-2021 strain, the complete genome was sequenced using the high-throughput sequencing method. The complete genome of the GS-2021 strain comprises 142,532 bp and encodes 88 open reading frames (ORFs) in unique long (UL) regions, unique short (US) regions, internal repeat sequences (IRS), and terminal repeat sequences (TRS) parts, respectively. The GC content in the whole genome of the GS-2021 strain is 73.61%, which is similar to that of other published PRV strains (Table 3). Compared with the complete genome sequences of other PRV strains, the GS-2021 strain showed the following homology: 99.96%, 99.94%, 99.91%, and 99.91% for Chinese PRV variant strains HN1201, HLJ8, JM, and hSD-1, respectively; 99.84%, 99.80%, 99.70%, and 99.49% for Chinese recombinant PRV strains JS-XJ5, JSY7, FJ, and JS-2020, respectively; 99.48%, 99.27%, and 98.60% for Chinese classical PRV isolates Fa, Ea, and SC, respectively; 97.31%, 97.11%, 96.20%, 96.11%, and 96.02% for foreign classical PRV strains Kolchis, Kaplan, Bartha, Becker, and NIA3, respectively (Table 4). However, the GS-2021 strain had higher homology with the HN1201 strain isolated in 2015, but it was significantly lower identity with the Bartha strain, suggesting that the PRV GS-2021 strain may originated from the HN1201 strain in Henan, China, 2015, through transportation across provinces.

Table 3. The GC content in genome sequences of the PRV reference strains used in this study.

Strain	Accession Number	Genome Sequence	T (%)	C (%)	A (%)	G (%)	G+C (%)
TJ	143642	143642	13.27	36.94	13.10	36.69	73.63
HeN1	141803	141803	13.26	36.96	13.05	36.73	73.69
JS-2012	145312	145312	13.29	36.78	13.21	36.73	73.50
HLJ8	142298	142298	13.22	36.91	13.08	36.79	73.70
GD-YH	146012	146012	13.17	36.83	13.07	36.93	73.76
HN1201	144173	144173	13.27	36.81	13.18	36.73	73.54

 doi:10.20944/preprints202503.1223.v2

JS-XJ5	141955	141955	13.22	37.05	12.99	36.75	73.79
HeNZM	144235	144235	13.33	36.61	13.09	36.98	73.58
JSY7	144315	143452	13.17	36.98	13.01	3684	73.82
FJ	142763	142763	13.19	36.86	13.43	36.52	73.38
hSD-1	143236	143236	13.25	36.88	13.12	36.75	73.63
SD18	143905	143905	13.24	36.87	13.10	36.79	73.66
JM	144046	144046	13.19	36.92	13.06	36.83	73.75
CD22	142472	142472	13.23	37.05	13.03	36.69	73.74
HLJPRVJ	143520	143520	13.29	36.93	13.10	36.69	73.61
HLJ-2013	142560	142560	13.23	36.95	13.09	36.73	73.67
JS-2020	143246	143246	13.27	36.88	13.10	36.74	73.62
SC	142825	142825	13.26	36.93	13.13	36.68	73.61
Ea	142334	142334	13.28	36.89	13.12	36.72	73.60
Fa	141930	141930	13.25	36.89	13.06	36.80	73.70
Kolchis	141542	141542	13.23	37.11	13.08	36.58	73.69
Bartha	137764	137764	13.19	36.98	13.10	36.73	73.71
Kaplan	140377	140377	13.22	37.05	13.10	36.63	73.68
Becker	141113	141113	13.15	37.00	13.11	36.74	73.74
NIA3	142228	142228	13.15	36.97	13.11	36.77	73.74

Table 4. Comparison of complete genome and *gB*, *gC*, *gD*, and *gE* gene sequences of the PRV GS-2021 with referenced strains.

Comparison with the PRV GS-2021 Strain	**Nucleotide Identities (%)**				
	Genome Sequence	***gB***	***gC***	***gD***	***gE***
Chinese PRV variant strains	99.59-99.96	99.90-100.00	99.90-100.00	99.80-100.00	99.70-99.90
Chinese classical PRV strains	98.40-99.48	99.30-99.80	96.90-99.70	99.50-99.70	99.70
Foreign classical PRV strains	96.02-97.31	98.40-98.50	94.90-96.30	98.90-99.30	97.70-98.0

Furthermore, the *gB*, *gC*, *gD*, and *gE* genes of the GS-2021 strain were amplified using PCR and then analyzed by comparing the sequences with those of PRV in the GenBank database (Table 2). The *gB*, *gC*, and *gD* genes of the GS-2021 strain shared a 100% nucleotide sequence identity with most of the PRV variant strains isolated from different regions in China (Table 4). However, the *gB*, *gC*, and *gD* genes shared more than 99.3% nucleotide sequence homology with Chinese classical PRV strains but exhibited less than 99.3% nucleotide sequence homology with foreign strains (Table 4). Additionally, the *gE* gene did not show 100% nucleotide sequence identity with Chinese variant strains (Table 4). Compared with earlier PRV strains from China and other countries, the gE protein of the Chinese PRV variant strains contains two aspartate (Asp, D) insertions at sites 48 and 496, respectively (Figure 4). Notably, two Aspartate (Asp) insertions were also detected in the gE protein of the PRV GS-2021 strain, and glutamate (Glu) at position 91 was replaced by glycine (Gly) (Figure 4). Therefore, these results show that the PRV GS-2021 might be a variant PRV strain.

 doi:10.20944/preprints202503.1223.v2

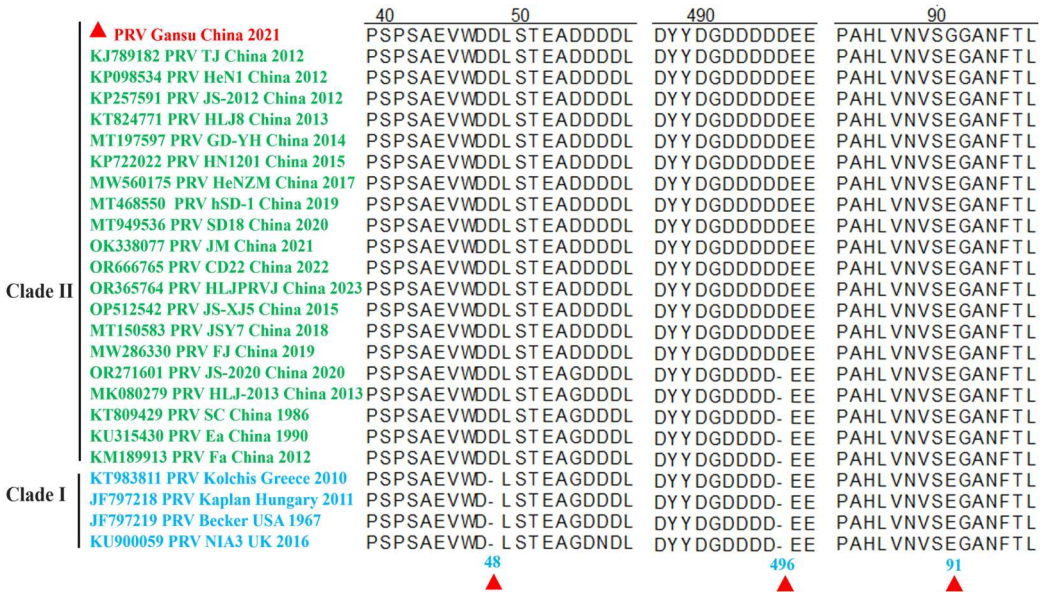

Figure 4. Comparative sequence alignment of PRV gE proteins. A total of twenty-five gE amino acid sequences of the PRV strains with complete genome sequences are available in GenBank and were compared using DNASTAR Lasergene 7 software. The sequences were aligned using the Clustal W method.

3.5. Phylogenetic Analysis of the PRV GS-2021 Strain

To investigate the phylogenetic relationship between the PRV GS-2021 strain and other PRV strains published in GenBank (Table 2), a phylogenetic tree was constructed based on the twenty-five complete genome sequences. The results of phylogenetic analysis show that the PRV strains are divided into two main evolutionary clades: clade I is composed of classical PRV strains from other countries, and clade II is composed of the PRV isolates from China, such as the Chinese classical PRV strains, the PRV variant strains and the recombinant PRV strains (Figure 5A). However, within clade II, the PRV GS-2021 strain is more closely related to the Chinese PRV variant strains and the recombinant PRV strains, including HN1201, HLJ8, hSD-1, JM, JS-XJ5, JSY7, FJ, and so on, than the Chinese classical PRV strains, such as Fa, Ea, and SC. Therefore, clade II is subdivided into two subclades, IIa and IIb. Clade IIa is composed of the Chinese classical PRV strains, and clade IIb is composed of the Chinese PRV variant strains and the recombinant PRV strains, which were responsible for the ongoing outbreak from 2012 to 2025 in China [12–15,19–23,33–41]. In addition, the phylogenetic tree of the twenty-five complete nucleotide sequences based on the gB, gC, gD, and gE genes also exhibited similar results (Figure 5B-D). Therefore, combining homology and phylogenetic analyses, the PRV GS-2021 strain was demonstrated to be a variant PRV isolate.

 doi:10.20944/preprints202503.1223.v2

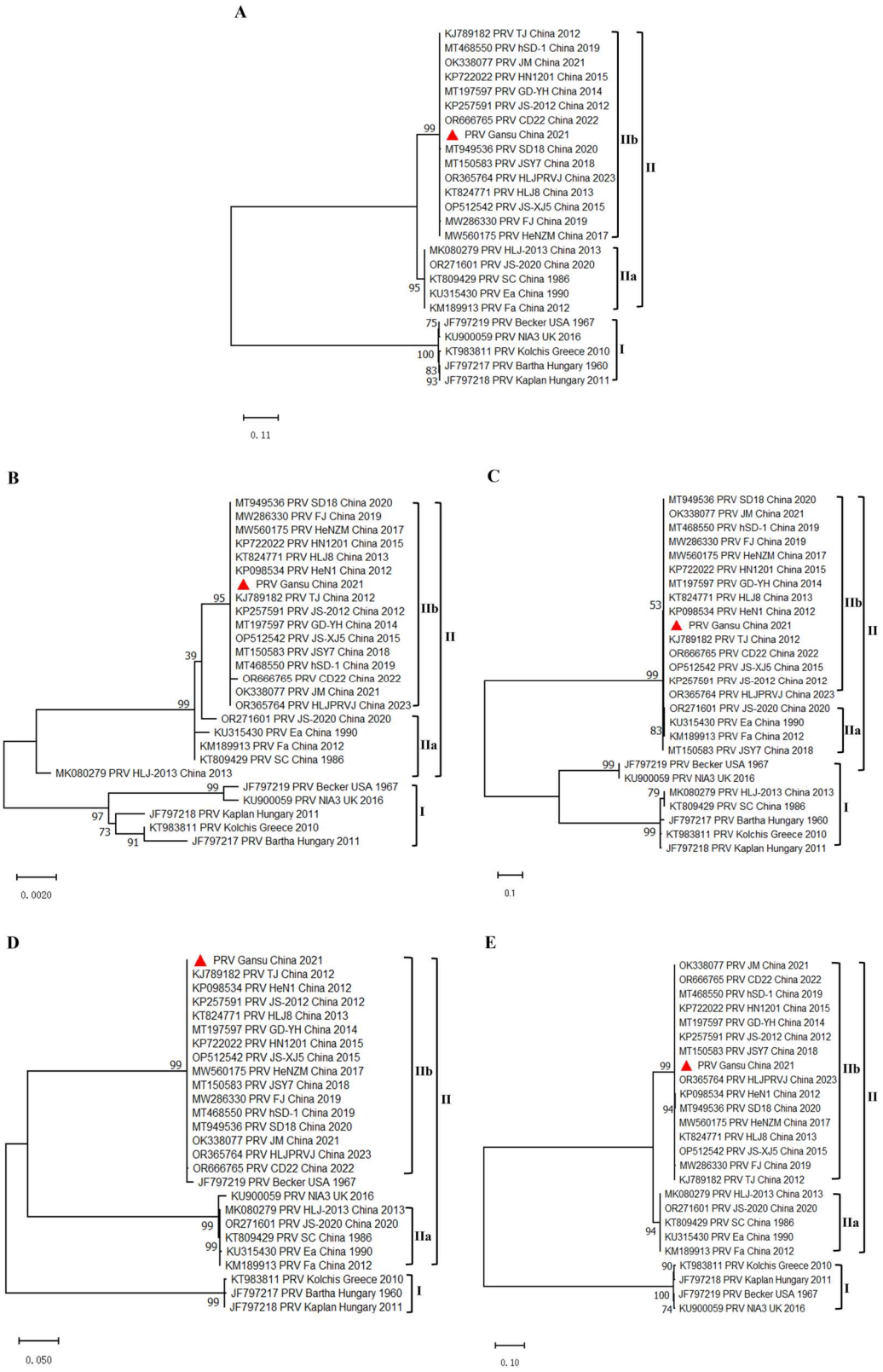

Figure 5. Phylogenetic analysis of the PRV strains. The phylogenetic trees based on the complete genomic sequences (A), *gB* (B), *gC* (C), *gD* (D), and *gE* (E) were constructed using the MEGA-X software with the ML method, bootstrapping with 1,000 replicates was performed to determine the percentage reliability for each internal node, and all branch lengths were drawn to a scale of nucleotide substitutions per site. The isolated PRV/Gansu/China/2021 strain is indicated by red triangle.

 doi:10.20944/preprints202503.1223.v2

3.6. Pathogenicity of the PRV GS-2021 Strain in Mice

To investigate the pathogenicity of the PRV GS-2021 strain, all mice were challenged intranasally with the PRV GS-2021 strain at doses of 10^4, 10^3, and 10^2 PFU/mice, respectively, with the Bartha-K61 vaccine strain and DMEM serving as controls. The results show that the GS-2021 strain was more lethal to all mice. The inoculated mice developed typical PRV symptoms, such as severe itching, convulsions, and acute death in 2-3 days. The death rate reached 100% (8/8) for 10^4 PFU and 10^3 PFU, and 37.5% (3/8) for 10^2 PFU (Table 5) (Figure 6A). The LD50 of the GS-2021 strain was $10^{2.125}$ PFU/0.01 ul, which is lower than that of the Bartha-K61 vaccine strain, $10^{5.75}$ PFU/0.01 ul (Table 5). However, all mice infected with the Bartha-K61 vaccine strain at 10^4 PFU did not show obvious clinical symptoms. At infection doses of 10^5 and 10^6 PFU, one (1/8, 12.5%) and five mice (5/8, 62.5%) died, respectively, on the 14th day post-inoculation (Table 5) (Figure 6A). Additionally, histopathologic examinations showed that the PRV GS-2021 strain caused multiple lesion sites in the liver, spleen, and lungs, including local necrosis, apoptosis, congestion, and the infiltration of lymphocytes (Figure 5B). Moreover, higher viral loads were detected in the blood, lungs, spleen, liver, and brain from mice infected with the PRV GS-2021 strain compared to the Bartha-K61 vaccine strain-infected group at 3 days post-infection (Figure 6C). In accordance with the gB-specific TaqMan qPCR results, the IFA also showed PRV-strong positive signals in the lungs, spleen, liver, and brain in the GS-2021 strain infected groups compared to the positive group and the mock group (Figure 6D). These results, therefore, suggest that the isolated PRV GS-2021 has higher pathogenicity in mice.

Table 5. The LD50 values of the PRV strains in BALB/c mice.

Group	Mice number in each group	Dose (PFU)	Mortality	LD50
GS-2021	8	10^4	8/8	$10^{2.125}$/0.01ul
	8	10^3	8/8	
	8	10^2	3/8	
Bartha-K61	8	10^6	5/8	$10^{5.75}$/0.01ul
	8	10^5	1/8	
	8	10^4	0/8	
DMEM	8	/	0/8	/

 doi:10.20944/preprints202503.1223.v2

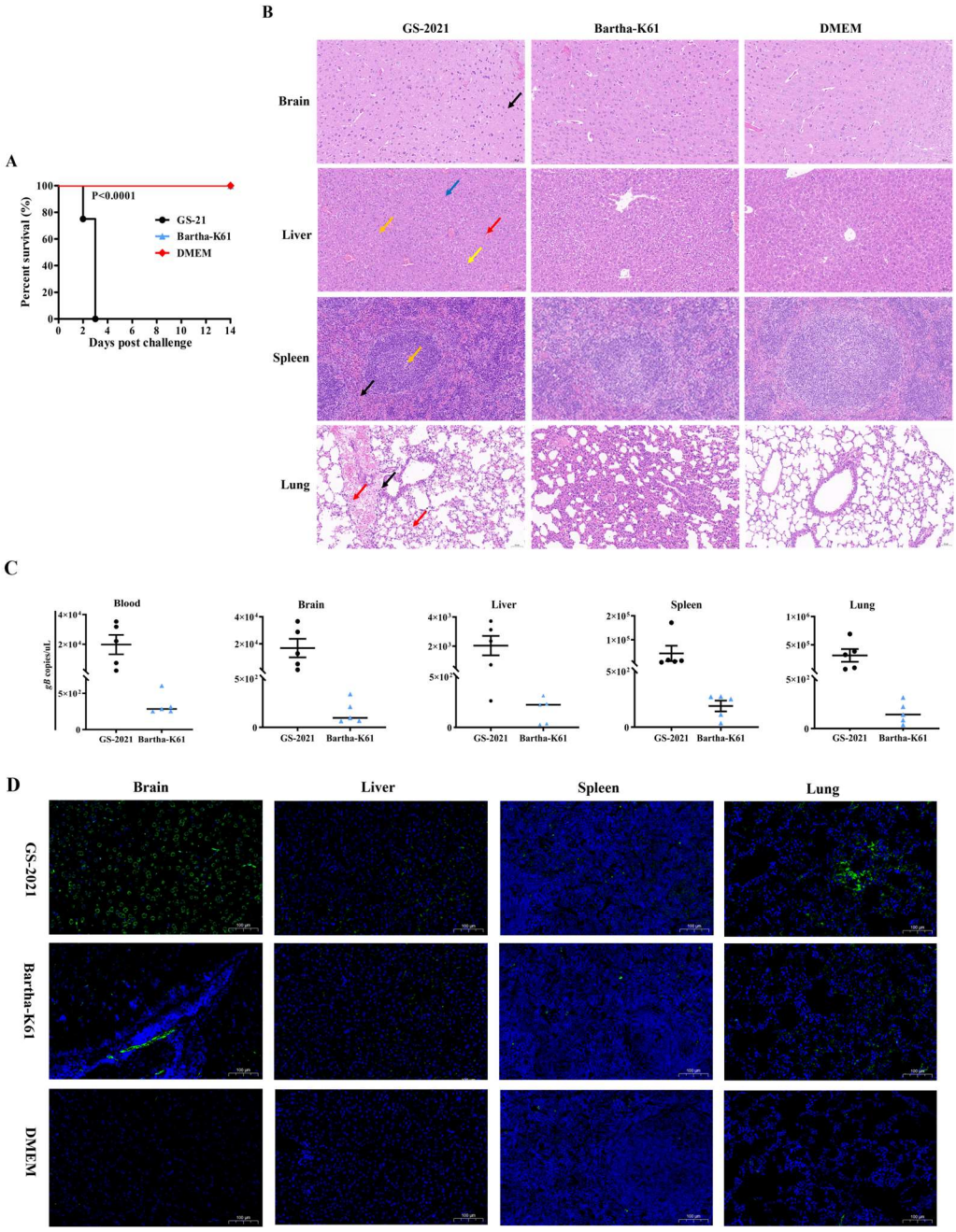

Figure 6. Pathogenicity analyses of the PRV GS-2021 strain in mice. (**A**) Kaplan–Meier survival curves of mice challenged with 10^4 PFU of GS-2021 and Bartha-K61 through intranasal routes (n=8 in each group). (**B**) Histopathological changes in different tissues of mice infected with GS-2021. Paraffin sections of brain, liver, spleen, and lung tissues from control, 10^4 PFU GS-2021, and 10^4 PFU Bartha-K61 groups were stained with hematoxylin and eosin (n=3 in each group). Infiltration of inflammatory cells (black arrows), hemorrhage (red arrows), local necrosis (orange arrows), vacuoles in the cytoplasm (yellow arrows), cell swelling, and cytoplasm vacuolar (blue arrows). (**C**) PRV *gB* gene copies in blood, brain, liver, lung, and spleen samples of the mice intranasally challenged by GS-2021 and Bartha-K61, determined using gB-specific TaqMan real-time PCR. Each dot represents 1 mouse, and the data were collected and presented as the means ± SEMs from 5 mice in each group. (**D**) Identification of viral particles in brain, liver, lung, and spleen tissues using IFA analysis (n=3 in each group). Anti-PRV polyclonal antibody was used as the primary antibody, and goat anti-rabbit IgG Alexa Fluor®488 (H+L) was used as the secondary antibody. The nucleus was stained with DAPI.

 doi:10.20944/preprints202503.1223.v2

4. Discussion

PRV is a widely spread, highly pathogenic virus that infects multiple domestic and wild animals and humans. Different isolated PRV virus strains exhibit varying virulence and biological characteristics, although they all belong to one strain type [1,23,24,52,53]. Since late 2011, several emerging PRV variants have been identified in Bartha-K61-vaccinated pig farms, with the variant strains rapidly spreading to most regions of China and causing significant economic losses to the swine industry in China [12–15]. Although the PRV inactivated and live-attenuated vaccines based on the variant strains have greatly contributed to the control of PR in the field, many reports have indicated that there was a high risk of substantial epidemics caused by the PRV variant or recombinant strains from 2012 to 2025, indicating the need for continuous monitoring of PR [12–15,17,19–23,33–41,52–56]. Therefore, further understanding the biological, genetic characteristics and pathogenicity of the prevalent PRV variant strains is important for preventing and controlling PR in China. However, there is ongoing debate regarding the PRV variant strains currently persisting in Gansu Province, China [57–59], as their biological characteristics, genetic features, evolutionary relationship, and pathogenicity are still unknown.

In the current study, a field PRV variant strain called PRV/Gansu/China/2021 (PRV GS-2021) was successfully isolated and identified from the PRV-suspected clinical brain tissue samples of dead piglets from a conventional Bartha-K61-vaccinated pig farm in Gansu Province, China in 2021, suggesting that the PRV variant strain was already circulating in Gansu Province before 2021. Moreover, one-step growth curves revealed that the isolated PRV variant strain had similar growth characteristics to Bartha-K61 vaccine strains in vitro, but it grew to high titers in Vero cells. In particular, the PRV GS-2021 strain propagated slightly slower than Bartha-K61 in PK-15 cells, suggesting that the Bartha-K61 strain has a better ability to adapt to this cell line. However, the plaque diameter of the PRV GS-2021 strain was significantly bigger than that of Bartha-K61 in Vero cells. The results show that the PRV GS-2021 strain had similar biological characteristics with previously isolated PRV variant strains. It is believed that several PRV infection cases in Gansu Province in recent years were also caused by PRV variant strains, including the PRV GS-2021 variant strain [57–59].

At present, the PRV strains prevalent worldwide are classified into clades I and II according to the phylogenetic and epidemiologic features. Clade I mainly contains classical PRV strains from most regions of Europe and America, whereas clades II contain classical and variant PRV strains and mainly prevalent in China [19,20,55,56]. The PRV variant strains are currently further classified into two sub-clades: clade IIa, also known as classical PRV strains, which were more common before 2011, and clade IIb, also known as novel PRV variants, which were first observed in late 2011 and since then have been dominant in China [19,20,55,56]. We found that the PRV GS-2021 strain belongs to clade II and is closely related to the variant strains in China (clade IIb) based on the *gB*, *gC*, *gD*, and *gE* gene sequences and the complete genome. As of now, it is believed that clade IIb remains the predominant epidemic clade affecting substantial economic losses in the pig industry in China, including Gansu Province. Meanwhile, we found PRV GS-2021 strain showed high homology with clades II, including Chinese PRV variant strains, but it showed low homology with clades I, including the Bartha-K61 vaccine strain, based on the nucleotide and amino acid sequence of the gB, gC, gD, and gE and the complete genome sequences of PRV. It is well known that the PRV gB, gC, and gD proteins are the major immunogenetic antigens that can induce neutralizing antibody production [45,60,61]. Therefore, these results provide a possible explanation for why the Bartha-K61 vaccine strain provides only partial protection for PRV variant infections. Interestingly, two Asp insertions as characteristic molecular markers of the PRV variant strains, are detected at sites 48 and 496 in the gE protein of the PRV GS-2021 strain. In contrast, only one Asp insertion is detected at site 48 in the gE protein of the Chinese classical PRV strains [12–15,19–23,61]. However, Glu is replaced by Gly at position 91 only in the gE protein of the PRV GS-2021 strain. These results suggest that the insertion and substitution events in the gE protein of the PRV variants are not coincidental phenomena and may be related to immune pressure in the host from the vaccine strain. Furthermore, they may cause changes in the pathogenicity and antigen characteristics of the PRV variant strains, including the PRV

 doi:10.20944/preprints202503.1223.v2

GS-2021 strain. Therefore, these results further explain why the Bartha-K6 vaccine strain provides ineffective protection against the PRV variant strains and why it is necessary to continuously monitor the epidemiological trend and genetic evolution of PRV in China.

Of note, more interspecies transmission events have been observed with clade IIb PRV in recent years including dog, tiger, foxes, minks, raccoons, bovine, sheep, and goat [1 – 6,19–22,62,63]. Importantly, a PRV variant strain called PRV/hSD-1/China/2019 was isolated from an acute human encephalitis case in 2019. This strain can effectively infect human cells and is genetically closest to those PRV variant strains currently circulating in pigs in China [50,51]. In addition, since 2017, some reports have shown that PRV might infect humans, as evidenced by the detection of nucleic acids for PRV using PCR and metagenomic next-generation sequencing or the detection of PRV-gE/gB-specific antibodies using ELISA in China [20–22,42–50]. These findings largely support the close phylogenetic relationship and similar etiological characteristics of PRV GS-2021 and hSD-1/2019 with other variant strains. This suggests that the PRV variant strain is an emerging zoonotic pathogen that can infect humans under conditions. It further highlights the significant risk of PRV variant strains transmitting from pigs to other animals, pigs to humans, humans to other animals, and humans to humans. However, further investigation is required to obtain more information regarding additional PRV variant strains derived from human infection cases. For example, it remains to be determined whether different PRV strains have different virulence and pathogenicity in humans and whether the current vaccines or antivirus drugs are safe and effective enough for humans to prevent novel PRV variants infections. Additionally, whether there is a correlation between PRV human infection cases and PRV infection levels in pigs remains unclear. Finally, whether the PRV GS-2021 strain can cross the species barrier and be transmitted to humans remains unknown.

The pathogenicity of the PRV GS-2021 strain was evaluated in mice in this study. All of the infected mice died by the 3rd day, and typical PRV-induced symptoms were observed when the mice were infected with 10^4 and 10^3 PFU of PRV GS-2021. Even when infected with 10^2 PFU of PRV GS-2021, three mice died by the 5th day after infection. In contrast, all mice infected with 10^4 PFU of the Bartha-K61 vaccine strain exhibited normal behavior by the 5th day post-infection, and no mice died by the end of the experiment on the 14th day. However, one and five mice died on the 14th day post-inoculation with infection doses of 10^6 and 10^5 PFU, respectively. In addition, the LD50 of the PRV GS-2021 strain was significantly lower than that of the Bartha-K61 vaccine strain, which has also been reported in previous studies [12–15,23,24,33–41,52–54,60–63]. This indicates that PRV GS-2021 could have higher virulence. PRV DNA and antigen-specific fluorescence signals were further detected in different tissue samples from the mice infected with 10^4 PFU of PRV GS-2021 within 3 days of post-infection. Moreover, the PRV GS-2021 strain infection in mice led to encephalitis in the brain, including meningeal congestion, hemorrhage, edema, and local necrosis. Histopathological examination revealed multiple lesion sites, including apoptosis, congestion, and the infiltration of lymphocytes in the liver, spleen, and lungs, suggesting that the extensive organ damage caused by PRV infection may have been the main cause of death in these mice. Regarding the underlying mechanism leading to damage in multiple organs, we speculate that the process begins at the site of PRV infection, where the virus first replicates. Then, it disseminates via the lymphatic system, and viraemia occurs when the virus is released into the bloodstream. This then leads to infection in the lungs, spleen, brain and other organs, where the virus replicates uncontrollably. This caused the mice to suffer multi-organ damage, and most of them died. Notably, histopathologic examinations were normal in all tissues of the Bartha-K61 vaccine strain-infected mice, which may be related to the infection route, dose, and time, the virulence of the virus strain, and the age of the animal model. Herein, we have further demonstrated that the PRV GS-2021 strain has higher virulence in mice. However, the pathogenicity of the PRV GS-2021 strain and other strains will require further evaluation in other animals, including pigs, bovine, sheep, and rhesus monkeys, in future studies.

 doi:10.20944/preprints202503.1223.v2

5. Conclusions

In summary, a PRV variant strain, called PRV/Gansu/China/2021 (PRV GS-2021), was isolated and identified from a Bartha-K61-vaccinated pig farm in Gansu Province, China in 2021. The PRV GS-2021 strain has higher virulence and pathogenicity, according to its etiological features, biological properties, phylogenetic relationships, and pathogenicity in mice in our study, and it may have already been circulating in Gansu Province before 2021. Our results provide a theoretical reference for better understanding of the epidemiological, genetic evolutionary patterns, characteristics and pathogenicity of PRV. These findings can contribute to novel vaccine designs, as well as the control, prevention, and eradication of the PRV epidemic in China.

Author Contributions: Conceptualization, Y.W. and Z.J.; methodology, X.H., H.Y., P.J., G.C., and Y.F.; software, X.H., P.J., and G.C.; validation, X.H. and H.Y.; formal analysis, X.H.; investigation, X.H., P.J., G.C., and Y.F.; data curation, X.H.; writing—original draft preparation, X.H.; writing—review and editing, X.H., P.J., Y.W., and Z.J.; visualization, X.H.; supervision, Y.W. and Z.J.; project administration, X.H. and H.Y; funding acquisition, X.H. and H.Y. All authors have read and agreed to the published version of the manuscript.

Funding: This work was funded by the Natural Science Foundation of Gansu Province (No. 20JR10RA018), the 2022 Innovation Fund Project of University Teachers (No. 2022B-357), and the Xinjiang Key Laboratory of Animal Infectious Diseases (No. 2023KLB003).

Institutional Review Board Statement: All animal experiments were handled in strict accordance with the Good Animal Practice Requirements of the Animal Ethics Procedures and Guidelines of the People's Republic of China, and the protocol was reviewed and approved by the Animal Ethics Committee of Lanzhou Veterinary Research Institute, Chinese Academy of Agricultural Science (Permission Number: LVRIAEC-2024-02-20).

Informed Consent Statement: Not applicable.

Data Availability Statement: The original contributions presented in the study are included in the article, and further inquiries can be directed at the corresponding authors.

Acknowledgments: We gratefully acknowledge Laboratory Animal Center of Lanzhou Veterinary Research Institute for raising animals. All the authors would like to acknowledge MDPI for English language editing (Certificate Number: 91452).

Conflicts of Interest: The authors declare no conflicts of interest. The funders had no role in the design of the study; in the collection, analyses, or interpretation of data; in the writing of the manuscript; or in the decision to publish the results.

References

1. Pomeranz, L.E.; Reynolds, A.E.; Hengartner, C.J. Molecular biology of pseudorabies virus: impact on neurovirology and veterinary medicine. *Microbiol. Mol. Biol. Rev.* **2005**, 69, 462–500.
2. Müller, T.; Hahn, E.C.; Tottewitz, F.; Kramer, M.; Klupp, B.G.; Mettenleiter, T.C.; Freuling, C. Pseudorabies virus in wild swine: A global perspective. *Arch. Virol*. **2011**, 156, 1691–1705.
3. Minamiguchi, K.; Kojima, S.; Sakumoto, K.; Kirisawa, R. Isolation and molecular characterization of a variant of Chinese gC-genotype II pseudorabies virus from a hunting dog infected by biting a wild boar in Japan and its pathogenicity in a mouse model. *Virus Genes* **2019**, 55, 322–331.
4. Liu, A.J.; Xue, T.; Zhao, X.; Zou, J.; Pu, H.L.; Hu X.L., Tian, Z.G. Pseudorabies virus associations in wild animals: Review of potential reservoirs for cross-host transmission. *Viruses* **2022**, 14, 2254.
5. Duan, S.H.; Li, Z.M.; Yu, X.J.; Li, D. Alphaherpesvirus in pets and livestock. *Microorganisms* **2025**, 13, 82.
6. Laval, K.; Enquist, L.W. The neuropathic itch caused by Pseudorabies virus. *Pathogens* **2020**, 9, 254.
7. Zhu, L.; Guo, W.Z.; Xu, Z.W. Fluctuant rule of colostral antibodies and the date of initial immunization for the piglets from sows inoculated with pseudorabies virus gene-deleted vaccine SA215. Chin. *J. Vet. Med*. **2004**, 24, 320–322. (In Chinese)

 doi:10.20944/preprints202503.1223.v2

8. He, Q.G.; Chen, H.C.; Fang, L.R.; Wu, B.; Liu, Z.F.; Xiao, S.B.; Jin, M.L. The safety, stability and immunogenicity of double genenegative mutant of pseudorabies virus strain (PRV HB-98). *Chin. J. Vet. Med*. **2006**, 26, 165–168. (In Chinese)
9. Chen, Q.Y.; Wu, X.M.; Che, Y.L.; Chen, R.J.; Hou, B.; Wang, C.Y.; Wang, L.B.; Zhou, L.J. The immune efficacy of inactivated Pseudorabies vaccine prepared from FJ-2012ΔgE/gI strain. *Microorganisms* **2022**, 10, 1880.
10. Sun, Y.; Luo, Y.; Wang, C.H.; Yuan, J.; Li, N.; Song, K.; Qiu, H.J. Control of swine pseudorabies in China: Opportunities and limitations. *Vet. Microbiol.* **2016**, 183, 119–124.
11. Freuling, C.M.; Müller, T.F.; Mettenleiter, T.C. Vaccines against pseudorabies virus (PrV). *Vet Microbiol*. **2017**, 206, 3-9.
12. Yu, X.L.; Zhou, Z.; Hu, D.M.; Zhang, Q.; Han, T.; Li, X.; Gu, X.X.; Yuan, L.; Zhang, S.; Wang, B.Y.; Qu, P.; Liu, J.H.; Zhao, X.Y.; Tian, K.G. Pathogenic pseudorabies virus, China, 2012. *Emerg. Infect. Dis.* **2014**, 20, 102–104.
13. An, T.Q.; Peng, J.M.; Tian, Z.J.; Zhao, H.Y.; Li, N.; Liu Y.M.; Chen, J.Z.; Leng, C.L.; Sun, Y.; Chang, D.; Tong, G.Z. Pseudorabies virus variant in Bartha-K61-vaccinated pigs, China, 2012. *Emerg. Infect. Dis.* **2013**, 19, 1749–1755.
14. Wu, X.M.; Chen, Q.Y.; Chen, R.J.; Che, Y.L.; Wang, L.B.; Wang, C.Y.; Yan, S.; Liu, Y.T.; Xiu, J.S.; Zhou, L.J. Pathogenicity and whole genome sequence analysis of a Pseudorabies virus strain FJ-2012 isolated from Fujian, Southern China. Can. J. Infect. Dis. *Med Microbiol*. **2017**, 2017, 9073172.
15. Luo, Y.Z.; Li, N.; Cong, X.; Wang, C.H.; Du, M.; Li. L.; Zhao, B.B.; Yuan, J.; Liu, D.D.; Li, S.; Li Y.F.; Sun, Y.; Qiu, H.J. Pathogenicity and genomic characterization of a pseudorabies virus variant isolated from Bartha-K61-vaccinated swine population in China. *Vet. Microbiol.* **2014**, 174, 107–115.
16. Gu, Z.; Dong, J.; Wang, J.; Hou, C.; Sun, H.; Yang, W.; Bai, J.; Jiang, P. A novel inactivated gE/gI deleted pseudorabies virus (PRV) vaccine completely protects pigs from an emerged variant PRV challenge. *Virus Res*. **2015**, 195, 57–63.
17. Tong, W.; Li, G.; Liang, C.; Liu, F.; Tian, Q.; Cao, Y.; Li, L.; Zheng, X.; Zheng, H.; Tong, G. A live, attenuated pseudorabies virus strain JS-2012 deleted for gE/gI protects against both classical and emerging strains. *Antivir. Res.* **2016**, 130, 110–117.
18. Hu, R.M.; Zhou, Q.; Song, W.B.; Sun, E.C.; Zhang, M.M.; He, Q.G.; Chen, H.C.; Wu, B.; Liu, Z.-F. Novel pseudorabies virus variant with defects in TK, gE and gI protects growing pigs against lethal challenge. *Vaccine* **2015**, 33, 5733–5740.
19. He, W.T.; Auclert, L.Z.; Zhai, X.F.; Wong, G.; Zhang, C.; Zhu, H.N.; Xing, G.; Wang, S.L.; He, W.; Li, K.M.; Wang, L.; Han, G.Z.; Veit, M.; Zhou, J.Y. Suo, G. Interspecies transmission, genetic diversity, and evolutionary dynamics of pseudorabies virus. *J. Infect. Dis.* **2019**, 219, 1705–1715.
20. Bo, Z.Y.; Li, X.D. A Review of pseudorabies virus variants: genomics, vaccination, transmission, and zoonotic potential. *Viruses* **2022**, 14, 1003.
21. Liu, Q.Y.; Kuang, Y.; Li, Y.F.; Guo, H.H.; Zhou, C.Y.; Guo, S.B.; Tan, C.; Wu, B.; Chen, H.C.; Wang, X.R. The epidemiology and variation in pseudorabies virus: a continuing challenge to pigs and humans. *Viruses* **2022**, 14, 1463.
22. Tan, L.; Yao, J.; Yang, Y.D.; Luo, W.; Yuan, X.M.; Yang, L.C.; Wang, A.B. Current status and challenge of pseudorabies virus infection in China. *Virol. Sin.* **2021**, 36, 588–607.
23. Yang, Q.Y.; Sun, Z.; Tan, F.F.; Guo, L.H.; Wang, Y.Z.; Wang, J.; Wang, Z.Y.; Wang, L.L.; Li, X.D.; Xiao, Y.; Tian, K.G. Pathogenicity of a currently circulating Chinese variant pseudorabies virus in pigs. *World J. Virol.* **2016**, 5, 23-30.
24. Wang, Y.; Xia, S.L.; Lei, J.L.; Cong, X.; Xiang, G.T.; Luo, Y.; Sun, Y.; Qiu, H.J. Dose-dependent pathogenicity of a pseudorabies virus variant in pigs inoculated via intranasal route. *Vet. Immunol. Immunopathol.* **2015**, 168, 147–152.
25. Zhou, J.Z.; Li, S.; Wang, X.B.; Zou, M.M.; Gao, S. Bartha-k61 vaccine protects growing pigs against challenge with an emerging variant pseudorabies virus. Vaccine **2017**, 35, 1161–1166.

 doi:10.20944/preprints202503.1223.v2

26. Wang, J.; Cui, X.; Wang, X.B.; Wang, W.B.; Gao, S.; Liu, X.F.; Kai, Y.; Chen, C.H. Efficacy of the Bartha-K61 vaccine and a gE-/gI-/TK- prototype vaccine against variant porcine pseudorabies virus (vPRV) in piglets with sublethal challenge of vPRV. *Res. Vet. Sci.* **2020**, 16-23.
27. Ren, Q.H.; Li, L.; Pan, H.C.; Wang, X.B.; Gao, Q.Q.; Huan, C.C.; Wang, J.; Zhang, W.; Jiang, L.Y.; Gao, S.; Kai, Y.; Chen, C.H. Same dosages of rPRV/XJ5-gI-/gE-/TK- prototype vaccine or Bartha-K61 vaccine similarly protects growing pigs against lethal challenge of emerging vPRV/XJ-5 strain. *Front. Vet. Sci.* **2022**, 896689.
28. Papageorgiou, K.V.; Michailidou, M.; Grivas, I.; Petridou, E.; Stamelou, E.; Efraimidis, K.; Chen, L.; Drew, T.W.; Kritas, S.K. Bartha-K61 vaccine protects nursery pigs against challenge with novel European and Asian strains of Suid herpesvirus 1. *Vet. Res.* **2022**, 53, 47.
29. Wang, T.; Xiao, Y.; Yang, Q.; Wang, Y.; Sun, Z.; Zhang, C.; Yan, S.; Wang, J.; Guo, L.; Yan, H.; Gao, Z.Y.; Wang. L.L.; Li, X.D.; Tan, F.F.; Tian, K.G. Construction of a gE-deleted Pseudorabies virus and its efficacy to the new-emerging variant PRV challenge in the form of killed vaccine. *BioMed Res. Int.* **2015**, 2015, 684945.
30. Zhang, C.; Guo, L.; Jia, X.; Wang, T.; Wang, J.; Sun, Z.; Wang, L.; Li, X.; Tan, F.; Tian, K. Construction of a triple gene-deleted Chinese Pseudorabies virus variant and its efficacy study as a vaccine candidate on suckling piglets. *Vaccine* **2015**, 33, 2432–2437.
31. Gao, J.F.; Lai, Z.; Shu, Y.H.; Qi, S.H.; Ma, J.J.; Wu, B.Q.; Gong, J.P. Isolation and identification of porcine pseudorabies virus (PRV) C strain. *Acta Agric. Shanghai* **2015**, 31, 32–36. (In Chinese)
32. Tang, Y.D.; Liu, J.T.; Wang, T.Y.; An, T.Q.; Sun, M.X.; Wang, S.J.; Fang, Q.Q.; Hou, L.L.; Tian, Z.J.; Cai, X.H. Live attenuated pseudorabies virus developed using the CRISPR/Cas9 system. *Virus Res.* **2016**, 225, 33–39.
33. Bo, Z.Y.; Miao, Y.Y.; Xi, R.; Gao, X.Y.; Miao, D.L.; Chen, H.; Jung, Y.Se.; Qian, Y.J.; Dai, J.J. Emergence of a novel pathogenic recombinant virus from Bartha vaccine and variant pseudorabies virus in China. *Transbound Emerg. Dis.* **2021**, 68, 1454-1464.
34. Tan L, Yao J, Lei L, Xu K, Liao F, Yang S, Yang L, Shu X, Duan D, Wang A. Emergence of a novel recombinant Pseudorabies virus derived from the field virus and its attenuated vaccine in China. *Front Vet Sci.* **2022**, 9, 872002.
35. Qin, Y.; Qin, S.; Huang, X.; Xu, L.; Ouyang, K.; Chen, Y.; Wei, Z.; Huang, W. Isolation and identification of two novel pseudorabies viruses with natural recombination or TK gene deletion in China. *Vet. Microbiol.* **2023**, 280, 109703.
36. Lian Z, Liu P, Zhu Z, Sun Z, Yu X, Deng J, Li R, Li X, Tian K. Isolation and characterization of a novel recombinant classical Pseudorabies virus in the context of the variant strains pandemic in China. *Viruses.* **2023**, 15, 1966.
37. Huang J, Zhu L, Zhao J, Yin X, Feng Y, Wang X, Sun X, Zhou Y, Xu Z. Genetic evolution analysis of novel recombinant pseudorabies virus strain in Sichuan, China. *Transbound Emerg Dis.* **2020**, 67, 1428-1432.
38. Huang J, Tang W, Wang X, Zhao J, Peng K, Sun X, Li S, Kuang S, Zhu L, Zhou Y, Xu Z. The Genetic Characterization of a novel natural recombinant Pseudorabies virus in China. *Viruses.* **2022**, 14, 978.
39. Jiang L, Cheng J, Pan H, Yang F, Zhu X, Wu J, Pan H, Yan P, Zhou J, Gao Q, Huan C, Gao S. Analysis of the recombination and evolution of the new type mutant pseudorabies virus XJ5 in China. *BMC Genomics.* **2024**, 25, 752.
40. Zhang, Z.D.; Wei, Q.T.; Wu, C.Y.; Ye, Z.Q.; Qin, L.T.; Chen, T.; Sun, Z.; Tian, K.G.; Li, X.D. Isolation and pathogenicity of a novel recombinant pseudorabies virus from the attenuated vaccine and classical strains. *Front. Vet. Sci.* **2025**, 12, 1579148.
41. Tan, L.; Zhou, Y.J.; Qiu, Y.X.; Lei, L.; Wang, C.; Zhu, P.; Duan, D.Y.; Lei, H.Y.; Yang, L.C.; Wang, N.D.; Yang, Y.; Yao, J.; Wang, W.; Wang, A.B. Pseudorabies in pig industry of China: Epidemiology in pigs and practitioner awareness. *Front. Vet. Sci.* **2022**, 9, 973450.
42. Ai, J.W.; Weng, S.S.; Cheng, Q.; Cui, P.; Li, Y.J.; Wu, H.L.; Zhu, Y.M.; Xu, B.; Zhang, W.H. Human endophthalmitis caused by pseudorabies virus infection, China, 2017. *Emerg. Infect. Dis.* **2018**, 24, 1087–1090.
43. Yang, X.; Guan, H.; Li, C.; Li, Y.; Wang, S.J.; Zhao, X.H.; Zhao, Y.Y.; Liu, Y.M. Characteristics of human encephalitis caused by pseudorabies virus: A case series study. *Int J Infect Dis.* **2019**, 87, 92-99.

 doi:10.20944/preprints202503.1223.v2

44. Wang, D.; Tao, X.G.; Fei, M.M.; Chen, J.; Guo, W.; Li, P.; Wang, J.Q. Human encephalitis caused by pseudorabies virus infection: a case report. *J Neurovirol*. **2020**, 26, 442–448.
45. Wong, G.; Lu, J.H.; Zhang, W.H.; Gao, G.F. Pseudorabies virus: a neglected zoonotic pathogen in humans? *Emerg. Microbes Infect.* **2019**, 8, 150–154.
46. Guo, Z.H.; Chen, X.X.; Zhang, G.P. Human PRV infection in China: an alarm to accelerate eradication of PRV in domestic pigs. *Virol. Sin.* **2021**, 36, 823-828.
47. Hou, Y.; Wang, Y.M.; Zhang, Y.; Yu, H.D.; Zhao, Y.; Yi, A.F. Human encephalitis caused by Pseudorabies virus in China: A case report and systematic review. *Vector Borne Zoonotic Dis.* **2022**, 22, 391-396.
48. Yan, W.Q.; Hu, Z. P.; Zhang, Y. C.; Wu, X.M.; Zhang, H.N. Case report: Metagenomic next-generation sequencing for diagnosis of human encephalitis and endophthalmitis caused by Pseudorabies virus. *Front Med (Lausanne)*. **2022**, 8, 753988.
49. Chen, Y.M.; Gao, J.; Hua, R.Q.; Zhang, G.P. Pseudorabies virus as a zoonosis: scientific and public health implications. *Virus Genes* **2025**, 61, 19–25.
50. Liu, Q.Y.; Wang, X.J.; Xie, C.H.; Ding, S.F.; Yang, H.N.; Guo, S.B.; Li, J.X.; Qin, L.Z.; Ban, F.G.; Wang, D.F.; Wang, C.; Feng, L.X.; Ma, H.C.; Wu, B.; Zhang, L.P.; Dong, C.X.; Xing, L.; Zhang, J.W.; Chen, H.C.; Yan, R.Q.; Wang, X.R.; Li, W. A novel human acute encephalitis caused by pseudorabies virus variant strain. *Clin. Infect. Dis.* **2021**, 73, e3690-e3700.
51. Peng, Z.; Liu, Q.Y.; Zhang, Y.B.; Wu, B.; Chen, H.C.; Wang, X.R. Cytopathic and genomic characteristics of a human-originated pseudorabies virus. *Viruses* **2023**, 15, 170.
52. Zheng, H.H.; Fu, P.F.; Chen, H.Y.; Wang, Z.Y. Pseudorabies virus: From pathogenesis to prevention strategies. *Viruses* 2022, 14, 1638.
53. Sehl, J.; Teifke, J.P. Comparative pathology of pseudorabies in different naturally and experimentally infected species-A review. *Pathogens* **2020**, 9, 633.
54. Cheng, X.J.; Cheng, N.; Yang, C.; Li, X.L.; Sun, J.Y.; Sun, Y.F. Emergence and etiological characteristics of novel genotype pseudorabies virus variant with high pathogenicity in Tianjin, China. *Microb. Pathog.* **2024**, 197, 107061.
55. Zhuang, L.L.; Gong, J.S.; Shen, J.Y.; Zhao, Y.; Yang, J.B.; Liu, Q.X.; Zhang, Y.; Shen, Q.P. Advances in molecular epidemiology and detection methods of pseudorabies virus. *Discov. Nano.* **2025**, 20, 45.
56. Zhai, X.F.; Zhao W.; Li, K.M.; Zhang, C.; Wang C.C.; Su, S.; Zhou, J.Y.; Lei, J.; Xing, G.; Sun, H.F.; Shi, Z.Y.; Gu, J.Y. Genome characteristics and evolution of pseudorabies virus strains in eastern China from 2017 to 2019. *Virol. Sin.* **2019**, 34, 601–609.
57. Shi, P.; Li, S.E.; He, W.; Liu Z.J.; Zhou, X.N.; Ma, Z.X.; Sun, Y.P. Investigation and prevention of Pseudorabies in pig farms in Qingyang, Gansu. *Gansu Anim Husbandry and Vet Med*. **2011**, 41, 5–6. (In Chinese)
58. Kang, W.B.; Song, J.G.; Zhou, F.; Xue, X.J.; Zhang, L.; Kang, X.H. Serological investigation and suggestions of prevention and control of pseudorabies in large-scale pig farms in Gansu Province. *Anim. Sci. Abroad* **2015**, 35, 50–52. (In Chinese)
59. Wang, M.J.; Wang, J.Q.; Cheng, X.L.; Wang, Y. Sero-epidemiological investigation on Pseudorabies in scaled swine farms in Tianshui city of Gansu Province. *China Anim Health Inspection* **2023**, 40, 15–18. (In Chinese)
60. Tang, Y.D.; Liu, J.T.; Wang, T.Y.; Sun, M.X.; Tian, Z.J.; Cai, X.H. Comparison of pathogenicity-related genes in the current pseudorabies virus outbreak in China. *Sci. Rep.* **2017**, 7, 7783.
61. Zhang, Z.; Wang, C.; Wu, C.; Wei, Q.; Ye, Z.; Wang, W.; Sun, Z.; Tian, K.; Li, X. Emergence and characterization of three Pseudorabies variants with moderate pathogenicity in growing pigs. *Microorganisms* **2025**, 13, 851.
62. Cheng, Z.L.; Kong, Z.J.; Liu, P.; Fu, Z.D.; Zhang, J.D.; Liu, M.D.; Shang, L.Y. Natural infection of a variant pseudorabies virus leads to bovine death in China. *Transbound Emerg. Dis.* **2020**, 67, 518-522.
63. Duan, Y.Q.; Liu, Ning.; Tan, L.; Gao, L.; Zhu G.Y.; Tao, Z.Z.; Liu, B.Y.; Wang, A.B.; Yao, J. Isolation and biological characterization of a variant pseudorabies virus strain from goats in Yunnan Province, China. Vet Res Commun. 2025, 49,149.

 doi:10.20944/preprints202503.1223.v2